

A Northern Sky Survey for TeV Gamma-ray Sources using the Tibet-III air shower array

M. Amenomori^a, S. Ayabe^b, D. Chen^c, S.W. Cu^d, Danzengluobu^e, L.K. Ding^d, X.H. Ding^g, C.F. Feng^f, Z.Y. Feng^g, X.Y. Gao^h, Q.X. Geng^b, H.W. Guo^e, H.H. He^d, M. He^f, K. Hibinoⁱ, N. Hottaⁱ, Haibing Hu^e, H.B. Hu^f, J. Huang^k, Q. Huang^g, H.Y. Jia^g, F. Kajino^l, K. Kasahara^m, Y. Katayose^e, C. Katoⁿ, K. Kawata^k, Labaciren^e, G.M. Le^o, J.Y. Li^f, H. Lu^d, S.L. Lu^d, X.R. Meng^g, K. Mizutani^b, J. Mu^h, K. Munakataⁿ, A. Nagai^p, H. Nanjo^q, M. Nishizawa^q, M. Ohnishi^k, I. Ohtaⁱ, H. Onuma^b, T. Ouchi^h, S. Ozawa^k, J.R. Ren^d, T. Saito^r, M. Sakata^d, T. Sasakiⁱ, M. Shibata^c, A. Shiomi^k, T. Shiraiⁱ, H. Sugimoto^s, M. Takita^k, Y.H. Tan^d, N. Tateyamaⁱ, S. Torii^t, H. Tsuchiy^d, S. Udo^k, H. Wang^d, X. Wang^b, Y.G. Wang^f, H.R. Wu^d, L. Xue^f, Y. Yamamoto^o, C.T. Yan^k, X.C. Yang^h, S. Yasueⁿ, Z.H. Ye^g, G.C. Yu^g, A.F. Yuan^e, T. Yudaⁱ, H.M. Zhang^d, J.L. Zhang^d, N.J. Zhang^f, X.Y. Zhang^f, Y. Zhang^d, Yi Zhang^d, Zhaxisangzhu^e and X.X. Zhou^g

The Tibet AS γ Collaboration

- (a) Department of Physics, Hirosaki University, Hirosaki 036-8561, Japan
- (b) Department of Physics, Saitama University, Saitama 338-8570, Japan
- (c) Faculty of Engineering, Yokohama National University, Yokohama 240-8501, Japan
- (d) Key Lab. of Particle Astrophys., Institute of High Energy Physics, Chinese Academy of Sciences, Beijing 100049, China
- (e) Department of Mathematics and Physics, Tibet University, Lhasa 850000, China
- (f) Department of Physics, Shandong University, Jinan 250100, China
- (g) Institute of Modern Physics, South West Jiaotong University, Chengdu 610031, China
- (h) Department of Physics, Yunnan University, Kunming 650091, China
- (i) Faculty of Engineering, Kanagawa University, Yokohama 221-8686, Japan
- (j) Faculty of Education, Utsunomiya University, Utsunomiya 321-8505, Japan
- (k) Institute for Cosmic Ray Research, the University of Tokyo, Kashiwa 277-8582, Japan
- (l) Department of Physics, Konan University, Kobe 658-8501, Japan
- (m) Faculty of Systems Engineering, Shibaura Institute of Technology, Saitama 337-8570, Japan
- (n) Department of Physics, Shinshu University, Matsumoto 390-8621, Japan
- (o) Center of Space Science and Application Research, Chinese Academy of Sciences, Beijing 100080, China
- (p) Advanced Media Network Center, Utsunomiya University, Utsunomiya 321-8585, Japan
- (q) National Institute of Informatics, Tokyo 101-8430, Japan
- (r) Tokyo Metropolitan College of Aeronautical Engineering, Tokyo 116-0003, Japan
- (s) Shonan Institute of Technology, Fujisawa 251-8511, Japan
- (t) Advanced Research Institute for Science and Engineering, Waseda University, Tokyo 169-8555, Japan
- (u) RIKEN, Wako 351-0198, Japan

Presenter: M. Sakata (sakata@konan-u.ac.jp), jap-sakat@M-abs1-og22-poster

Using the Tibet III air shower array data (Nov. 1999~Oct. 2004) a wide survey for point sources of TeV gamma-ray was performed. Significant excesses from the well known steady source Crab Nebula and the flare type source Markarian 421 are observed, but no new source was found with sufficiently high significance. In addition to this search we obtained the low upper limits on the gamma-ray flux above 3 TeV and 10 TeV for the declination band 0 degree through 60 degrees.

1. Introduction

Extensive Air Shower (EAS) experiments, such as the Tibet air shower array experiments, have observed gamma-ray emissions from standard candle Crab nebula and from transient sources such as Mrk501 and Mrk421 [1] [2][3]. Their characteristic abilities in high duty cycle and large field of view allow them to simultaneously monitor a larger area in space over continuous time. AIROBICC made a northern sky survey [4] for energies above 15 TeV, and obtained flux upper limit between 4.2 and 8.8 Crab for a declination of

0° and 60° . Most recently, Milagro updated its results [5] in the northern sky survey in TeV energy range, and pushed the average flux upper limit down to a level between 275 and 600 mcrab that is 4.80×10^{-12} to $10.5 \times 10^{-12} \text{ cm}^{-2} \text{ s}^{-1}$ above 1 TeV for source declinations between 5° and 70° . The Tibet III air shower array has similar sensitivity, and covers almost the same energy ranges and field of view as of those experiments. Recent results [6] and new one from the Tibet III air shower array will provide information for crosschecking and confirmation.

2. Experiment

The Tibet III air shower array settled at Yangbajing (90.522°E , 30.102°N ; 4,300m a.s.l) in Tibet [7], covering an area of $22,050 \text{ m}^2$. The array is composed of 533 scintillation counters of 0.5 m^2 in area and 3 cm in thickness, and is equipped with a fast-timing (FT) photomultiplier tube (PMT; Hamamatsu H1161). A 0.5 cm thick lead plate is put on the top of each counter in order to increase the array sensitivity by converting gamma-rays into electron-positron pairs in the shower. The angular resolution is about $0.9'$ in the energy region above 3 TeV, as estimated from full Monte Carlo (MC) simulation [8] and verified by the moon shadow measurement from observational data [3]. The trigger rate is higher than 680 Hz depending on running phases. The observational period was 1041 days from Nov. 1999 to Oct. 2004. The event selection was done by imposing the following four criteria on the reconstructed data: i) each shower event should fire four or more Fast-Time (FT) detectors recording 1.25 or more particles; ii) the estimated shower center location should be inside the array; iii) the sum of the number of particles per m^2 detected in each detector should be larger than 15; iv) the zenith angle of the incident direction should be less than 40° . After applying these cuts and a data quality cut, about 25% of the shower events were selected, results in a total number of events to be about 1.46×10^{10} .

3. Analysis

The number of background events was estimated from the event densities in the side band windows of each on-source window. Sitting on an almost horizontal plane, the Tibet III array has almost azimuth-independent efficiency in receiving the shower events for any given zenith angle. The equi-zenith angle method was therefore developed. In brief, simultaneously collected shower events in the same zenith angle belt can be used to construct the "off-source windows" and to estimate the background for a candidate point source located in the same zenith angle. The steady effects lead to an approximately 2.5% higher event rate from the southerly direction than from the northerly direction. This non-uniformity is properly accounted for in the following analyses.

For the purpose of crosschecking, two independently developed analyses based on the equi-zenith angle method are used in this work. The number of the background events estimated by the two methods is different due to the different ways used in choosing the off-source windows as seen in the subsections below. As a result, significance values calculated from the two methods differ by about 0.5 σ statistically.

Method I (short distance equi-zenith angle method) (a) Calculate approximate background level N_{BG}^* by average of ten N_{off} 's, on the base of Equi-Zenith-angle condition. (b) Correct small deviation due to many factors such as effects of non-observation periods, a slight slope (1.26 deg.) of the array ground and geomagnetic field may violate the equi-zenith uniformity. The correction factor R is given by N_{on} to N_{off} ratio with high statistics using 35 dummy-on directions having the same declination as the on-source. The exact background N_{BG} is given by $R N_{\text{BG}}^*$, and significance value S is calculated by $(N_{\text{ON}} - N_{\text{BG}}) / (1.0637 N_{\text{BG}}^{-1/2})$ where factor 1.0637 is necessary to estimate exact amount of fluctuation caused from all values used for the estimation of N_{BG} .

Method II (all distance equi-zenith angle method.) (a) To explore all of the statistic in background

estimation, the whole region of equi-zenith belt other than on-source window are taken as off-source window. Then large scale anisotropy of cosmic ray intensity has to be taken into account. (b) Denote $I_{on,off}$ as the flux intensities for on(off)-source windows, $N_{on,off}$ as the observed event number from on(off)-source window, N_{on}/I_{on} and N_{off}/I_{off} are then comparable to the N_{on}, N_{off} for Method I. (c) To determine the intensity of cosmic ray I , A χ^2 function comparing N_{on}/I_{on} against the averaged N_{off}/I_{off} is thus built for every on-source window at time t . For all direction and all moment, we can get all χ^2 function and then sum of them as total χ^2 . by minimizing this χ^2 function, and we can get CR relative intensity at all directions. The detail of this method was presented in Cui et al.[9].

4. Results

Significance distributions are obtained by the two methods as shown in Figure 1. while in general two shapes are in good agreement, small difference is seen in the highest significance region which may be caused by the different ways used in estimation of background for the two methods. Solid lines in both figures show the significance distribution. Dashed curves present normal Gaussian distribution. Excess from the Gaussian distribution is seen in the high significance region. When we omit significance values of windows whose centers are included inside circles of radius 2° centered at both directions of Crab and Mkn421, this excess disappear as shown by the thin-line histogram in Figure 1.

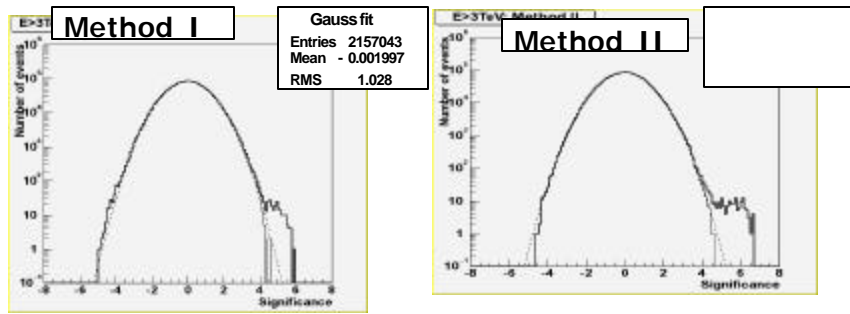


Figure 1. Significance distributions of all directions on the sky map from Method I and Method II. Solid lines in both figures are derived from all cells defined in analyses. Histograms of thin lines excludes those cells, centers of which have distances to Crab or Mrk421 of shorter than 2° . The dashed histogram represents the normal Gaussian distribution.

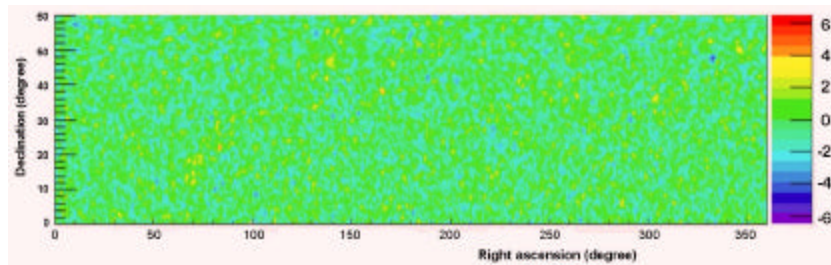


Figure 2. Map of significance distribution by Tibet III (1999~2004) given by Method I. Window size of each bin is of radius 0.9° . Two directions with significance greater than 5 sigma are Crab (left) and Mrk421(right).

Then this excess is well explained by the contributions of Gamma-rays from Crab and Mkn421 which was in an active state from Feb. 2000 through Oct. 2001 [3], and there is no other distinguished direction which has so large significance values that significance distributions deviate from the normal

Gaussian distributions. The two dimensional map of significance distribution in the sidereal coordinate is shown in Figure 2, in which two directions with high significance are Crab (left, 5.75σ) and Mrk421(right, 5.96σ). It should be noted that other high significances directions seen in the figure are, so far, consistent with statistical fluctuation. Flux upper limit at 90% confidence level for point source gamma-ray flux is calculated following the statistic method given by Helene [10]. The effective detection area of Tibet III air Shower array is evaluated by full M.C. simulation assuming a Crab-like gamma-ray spectrum of power -2.6. Figure 3 shows the average flux upper limit along the right ascension direction as a function of declination, which varies between $1.1-2.3 \times 10^{-12} \text{ cm}^{-2}\text{s}^{-1}$ for gamma-ray energy greater than 3 TeV which correspond to about 0.26-0.53 Crab, and $1.5-3.3 \times 10^{-12} \text{ cm}^{-2}\text{s}^{-1}$ (about 2.5-5.5 Crab) for greater than 10 TeV.

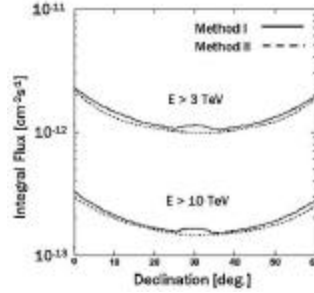


Figure 3. Declination dependence of 90% C.L. upper limits of gamma-ray integral flux above 3 TeV (upper lines) and 10 TeV (lower lines).

5. Conclusions

A northern sky survey for the TeV gamma-ray point sources in a declination band between 0° to 60° was performed using data of the Tibet III air shower array obtained from 1999 to 2004 with two independently developed analysis methods. The established Crab and Mrk421 were observed with high significance values of greater than 5 sigma, and no clear candidate for point source was found in the northern sky by our data set of these years. With the exception of Crab and Mrk421, 90% C.L. flux upper limits are obtained from the rest of the positions under the hypothesis that a candidate point source are in power law spectra, with indices varying from 2.6. The integral flux limits lie within depending on the declination band and power law index of the candidate source. Thus the upper limits was obtained as $1.1-2.3 \times 10^{-12} \text{ cm}^{-2}\text{s}^{-1}$ for gamma-rays with energy greater than 3 TeV, and $1.5-3.3 \times 10^{-12} \text{ cm}^{-2}\text{s}^{-1}$ for greater than 10 TeV.

6. Acknowledgments

This work is supported in part by Grants-in-Aid for Scientific Research on Priority Areas (712) (MEXT) and by Scientific Research (JSPS) in Japan, and by a grant for International Science Research from the Committee of the Natural Science Foundation and the Chinese Academy of Sciences in China.

References

- [1] Amenomori et al. 1999, ApJ, 525, L93
- [2] Amenomori et al. 2000, ApJ, 532, 302
- [3] Amenomori et al. 2003, ApJ, 598, 242
- [4] Aharonian et al. 2002, AAP, 390, 39
- [5] Atkins et al. 2004, ApJ, 608, 680-685
- [6] Amenomori et al. 2005, astro-ph/0502039
- [7] Amenomori et al. 2001, Proc. 27th Int. Cosmic Ray Conf. (Hamburg), 2, 573
- [8] Kasahara 2003, <http://cosmos.n.kanagawa-u.ac.jp/EPICSHome/>
- [9] Cui et al. 2003, Proc. 28th Int. Cosmic Ray Conf. (Tsukuba), 4, 2315.
- [10] Helene, O., 1983, Nucl. Instrum. Methods Phys. Res., 212, 319